Contents lists available at ScienceDirect

Colloids and Surfaces B: Biointerfaces

Full Length Article

Is the biocompatibility of copper with polymerized natural coating dependent on the potential selected for the electropolymerization process?

M. Bertuola [a], C.A. Grillo [a], D.E. Pissinis [a], E.D. Prieto [a], M. Fernández Lorenzo de Mele [a,b,*]

[a] Instituto de Investigaciones Fisicoquímicas Teóricas y Aplicadas (INIFTA, CONICET, UNLP), Facultad de Ciencias Exactas, Departamento de Química, Universidad Nacional de La Plata, Casilla de Correo 16, Sucursal 4, 1900 La Plata, Argentina
[b] Facultad de Ingeniería, Universidad Nacional de La Plata, Calle 47 y 1, 1900 La Plata, Argentina

ABSTRACT

With the intention of taking care of the environment and human health, the development of alternative eco-friendly methods to inhibit metal corrosion is intensively encouraged. In previous works we showed that some phytocompounds components of essential oils such as carvacrol (Carv) and thymol (TOH) are able to be electropolymerized on metals and they seem to be promissory for this purpose.

The aim this paper is to investigate if the biocompatibility of copper covered by coatings formed by electropolymerization of Carv and TOH (polyCarv and polyTOH) is related with the potential selected for the electropolymerization process. Potentiostatic perturbations at different potentials, AFM images, ATR-FTIR spectroscopy and measurements of copper ions release provided suitable information to make a detailed analysis of different stages of the electropolymerization process that leads to polyCarv and polyTOH layers on copper surface. The change of the characteristics of the coatings over time was evaluated after several polymerization periods and current transients were interpreted by using nucleation and growth models. Results showed interesting changes in the polymerization process with the electrochemical perturbation, nature of the isomer, and time of the treatment. The treatment that provides the most protective, transparent and homogeneous layer, that strongly increased the biocompatibility of Cu could be selected: electropolymerization of Carv at 0.4 V. Results highlight the importance of the detailed study of the evolution of the electropolymerization processes to select the best ecofriendly condition due the high impact of potential perturbation and polarization time on the biocompatibility of the resulting polymeric layer-copper system.

© 2017 Elsevier B.V. All rights reserved.

1. Introduction

Copper and its alloys are extensively used for diverse applications owing to their advantageous mechanical, thermal and conductivity properties together with their simple fabrication and joining. Additionally they are resistant to corrosion and biofouling and very suitable for piping, tubing, condensers and heat exchangers [1,2]. From environmental point of view their high recyclability and prolonged service life are also advantages [3–5]. On the other hand, due to their high conductivity and after accurately shielding, copper can be used to carry signals to small implants of diagnostic devices into the body.

However, copper-based metals are susceptible to corrosion in chloride-containing media [6–8] that are frequent in industrial and medical environments. Corrosion is detrimental both, owing to the economical costs involved in substitution or repair of the copper-containing devices and to the release of copper ions associated to the corrosion process that contaminates aqueous environments [9] and represents a potential risk for biological systems [10].

Coatings have been proposed in order to act as insulators to mitigate current transfer between anodic and cathodic areas and to obstruct the diffusion of oxygen and chloride towards copper surface. Several organic inhibitors have been suggested to hinder copper dissolution by adsorbing on copper surface. Some of them form self assembled monolayers (SAMs) on the metal sur-

* Corresponding author at: Instituto de Investigaciones Fisicoquímicas Teóricas y Aplicadas (INIFTA, CONICET, UNLP), Facultad de Ciencias Exactas, Departamento de Química, Universidad Nacional de La Plata, Casilla de Correo 16, Sucursal 4, 1900 La Plata, Argentina.

E-mail addresses: mbertuola@inifta.unlp.edu.ar (M. Bertuola), cgrillo@inifta.unlp.edu.ar (C.A. Grillo), dpissinis@gmail.com (D.E. Pissinis), tatiprieto@gmail.com (E.D. Prieto), mmele@inifta.unlp.edu.ar, fernandezlorenzom@hotmail.com (M. Fernández Lorenzo de Mele).

face [11,12]. Besides, hetero-cycles that are added to the corrosive solution can adsorb on copper and inhibit metal corrosion [13–19]. However, their impact on the environment is rarely evaluated notwithstanding the possible emergent risks.

With the aim of caring the environment, alternative eco-friendly methods, i.e. those that are not harmful to the environment, have been recently developed [20]. Natural compounds such as essential oils obtained from oregano and thyme show several advantages because they are low-cost, easily available and renewable. Importantly, they can be extracted inexpensively by simple procedures. On this respect, in a recent report [21] the fundamentals and recommended actions in decision-making to select eco-friendly procedures considering product design, manufacturing and usage phases for the succeeding product generation are discussed. In the case of oregano, among the several ways to produce the essential oil (supercritical fluid, solvent, water distillation), water distillation with full energy integration was selected as the better technology. The cost of oregano production by this procedure is 8.64 U$S/kg, close to the price of other synthetic corrosion inhibitors, but with a distinctive advantage: a low environmental impact is associated with this production (Potential environmental impact (PEI) 0.018 PEI/kg) and carbon footprint (0.80 kg CO_2-e/kg oil) for water distillation technology [22].

In a previous paper [23] we informed that the use of some phytocompounds seems to be suitable for corrosion inhibition. Thus, two of the components of *Origanum vulgare* and *Thymus vulgaris* essential oils, carvacrol (Carv) and thymol (TOH), were proposed as appropriate for the development of an eco-friendly treatment. They are also well known as antibacterial and antioxidant compounds [24]. The electrochemical results obtained by cyclic voltammetry showed that these phenolic isomers are able to electropolymerize on the metal surface. However, the characteristics of the layers should be optimized in order to improve biocompatibility and corrosion inhibition. A meticulous study of the process is imperative to select the best conditions.

The aim this paper was to investigate if the biocompatibility of copper covered by coatings formed by electropolymerization of Carv and TOH is related with the potential selected for the electropolymerization process. A detailed analysis of different stages of the process was made using potentiostatic polarization at several potentials and polarization periods. The change of the characteristics of the coatings over time was evaluated by AFM images, by measurements of copper ions release and by ATR-FTIR spectroscopy of the polyCarv and polyTOH layers. Current transients were interpreted by using nucleation and growth models. Proliferation of cells in the vicinity of the coated metal samples was examined to find the relationships between biocompatibility and the selected potentials used for the electropolymerization process.

2. Experimental section

2.1. Materials

Carvacrol (Carv) (Sigma, St. Louis, MO, USA), and Thymol (TOH) (Sigma, St. Louis, MO, USA) were used in the experiments. All chemicals employed in the assays were of analytical grade and ultrapure water was employed to prepare the solutions.

Cylindrical copper bars (99.7% electrolytic metal copper, 9 mm diameter) (Merck, Darmstadt, Germany) were used for electrochemical experiments and copper sheets (99.7%, 0.1 mm thick, 6 mm diameter) were used for biological experiments. These discs and bars were washed with (5% v/v) H_2SO_4, vigorously rinsed with ultrapure water and then dried with nitrogen.

2.2. Cu samples and generation of electropolymerized layers

Cylindrical copper bars, whose lateral surfaces were covered with polyoxymethylene, leaving an exposed area of 0.626 cm^2 were used as working electrodes for electrochemical experiments. Each electrode was mechanically polished with emery papers of different grain sizes using water as lubricant and then washed with water and ethanol, and dried with nitrogen. The electrode surface was carefully observed under optical microscope (Olympus BX51, Olympus Corp., Tokyo, Japan), before and after the experiments, to evaluate possible changes in color and/or texture of copper surface.

Electrochemical assays were made in a conventional electrochemical cell. A platinum foil was used as counter electrode and a saturated calomel electrode (SCE) as reference electrode. The potential values in the text are referred to the SCE.

Electropolymerized films of Carv and TOH (polyCarv and polyTOH) on copper (sheets or cylinders) were attained by potentiostatic electrochemical methodology (Chronoamperometric measurements, CA) by modifying that reported by Guenbour et al. [25,26]. The potential range was selected according to the electrooxidation region (0.20 V-0.55 V potential region) characterized by cyclic voltammetry (Fig. S1, Supplementary information). Potentiostatic steps from the open circuit potential (OCP) to the selected potential were made. 0.1 M Carv or 0.1 M TOH water/ethanol (70:30) alkaline solution (0.3 M NaOH) [25–27] was used as electrolyte for this treatment. The presence of EtOH in Carv solutions is necessary to improve Carv solubility.

Each test was run in triplicate to verify the reproducibility of the data. In all cases a potentiostat-galvanostat TEQ03 was used.

2.3. Measurement of copper ions release

The copper ions released from the discs covered by polyCarv or polyTOH films after their immersion in 3 ml of 0.136 M KCl solution for 6 days at room temperature was measured by colorimetric analysis and by atomic absorption spectroscopy. Colorimetric method is based on the addition of 1-(2 pyridylazo)-2-naphthol (PAN) to the samples. This dye forms coloured complexes with a large number of metal ions, including Cu(II) which are suitable for spectrophotometric analysis. Briefly, an appropriate volume of H_2SO_4 was added to each sample to reach a final concentration of 0.25 M. An aliquot of 100 μl of these acidic samples was mixed with 100 μl of 4 mM PAN ethanolic dissolution and 800 μl of water. The absorbance was measured in a Shimadzu UV 1800 spectrometer at λ=560 nm, maximum of the absorption spectra of the Cu(II)−PAN complex. The copper content in an unknown sample was determined by comparing with a calibration curve [28].

The concentration of soluble copper in case of the bare copper was also determined by Flame atomic absorption spectrometer (Shimadzu AA-7000, Kyoto, Japan) after total dissolution with 1 ml 0.28 M nitric acid. Hollow cathode lamps were used as radiation sources (limit of detection = 0.02 μg/ml, obtained using internal quality control, according to standard procedures).

2.4. Surface analysis by ATR-FTIR and AFM

ATR-FTIR spectra were obtained in a Varian 660 spectrometer equipped with an attenuated total reflection (ATR) accessory (MIRacle ATR, Pike technologies) with a ZnSe prism. In all cases, each spectrum was the result of 256 scans taken with a resolution of 2 cm^{-1}.

Tapping® mode AFM (Nanoscope V; Bruker, Santa Barbara, CA) in topographic mode was used to characterize the substrates, using silicon tips (Arrow™ NCR; NanoWorld, Neuchâtel, Switzerland) (spring constant, 42 N/m; resonance frequency,
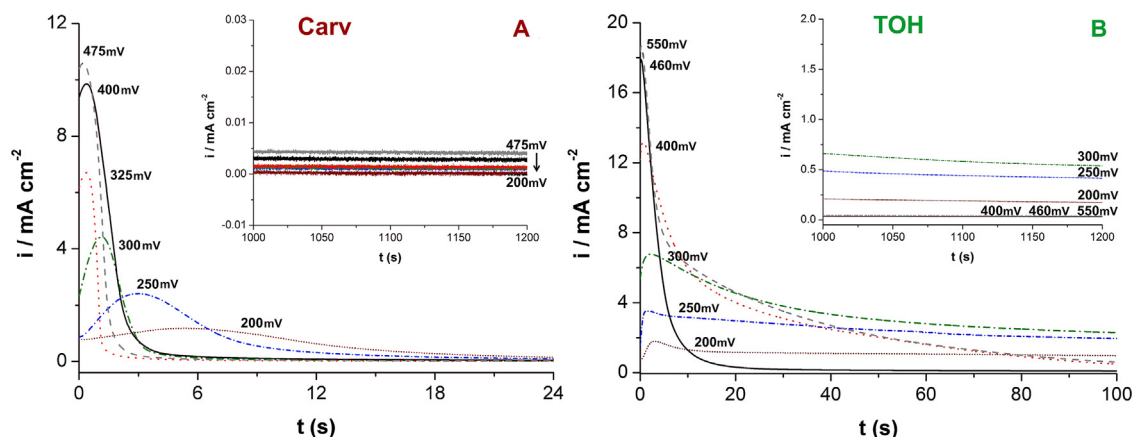
Fig. 1. Chronoamperometric measurements at constant potentials in the 200 mV to 550 mV (SCE) potential range in 0.3 M NaOH 70/30 with 0.1 M Carv (A) and 0.1 M TOH (B) water/EtOH solutions.

285 kHz). Nanoscope 7.30 and Nanoscope Analyis 1.5 softwares were employed to obtain the images (Bruker).

2.5. Biological assays

MC3T3-E1 is an osteoblast precursor cell line derived from *Mus musculus* (mouse). It was originally obtained from American Type Culture Collection (ATCC) (Rockville, MD, USA). Cells were grown as monolayer in T-25 flasks with DMEM culture medium (GIBCO-BRL, LA, USA) supplemented with 10% inactivated fetal calf serum (Natocor, Carlos Paz, Córdoba, Argentina), 50 IU/ml penicillin and 50 μg/ml streptomycin sulfate, (complete culture medium: CCM) at 37 °C in a 5% CO_2 humid atmosphere. Cells were counted in an improved Neubauer haemocytometer and viability was determined by the exclusion Trypan Blue (Sigma, St. Louis, MO, USA) method; in all cases viability was higher than 95%.

Colony formation assay or clonogenic assay is an *in vitro* cell survival assay based on the ability of a single cell to grow into a colony [29]. For this analysis cells were grown at 37 °C in 5% CO_2 humid atmosphere in CCM in presence of pure Cu discs (obtained from Cu sheets, 6 mm diameter) with and without surface treatment in the center of each Petri dish. An additional cell culture, growing without disc, was used as control. After 6 days incubation, colonies were stained with Acridine Orange dye (Sigma, St Louis, MO, USA) and immediately examined by epifluorescence microscopy (Olympus BX51, Olympus Corp., Tokyo, Japan) equipped with an appropriate filter, connected to an Olympus DP73 color video camera (Olympus Corp., Tokyo, Japan). Images were taken immediately after opening the microscope shutter to the computer monitor and then the diameter of colonies was measured with Image J software. The colonies were scored in two regions: A (close ≤18 mm) and B (distant to the disc; >118 mm). Three experiments were performed in independent trials to assess reproducibility. The number of colonies per experimental point was obtained. Statistical analysis was performed using χ^2 in case of the number of colonies and one-way ANOVA for the diameter of colonies.

3. Results and discussion

3.1. Chronoamperometric records

Chronoamperometric measurements were made at different potentials. In order to select the potential range, potentiodynamic polarization records in the 0.3 V–1.0 V potential range (Fig. S1) were obtained for Carv and TOH in water/ethanol (70:30) alkaline solution (0.3 M NaOH).

In view of the potentiodynamic electrochemical response (see Fig. S1 description), 0.2 V–0.55 V was chosen as potential region for potentiostatic current transients. Chronoamperometric records obtained with Carv showed sharp peaks at potentials close to the current peak of Fig. S1 (300 mV–475 mV) with maxima that reached more than 10 mAcm^{-2} after less than 1 s (400 mV, Fig. 1A). Subsequently current values decreased to very low values (a few μAcm^{-2}). For the more cathodic potentials assayed (200 mV and 250 mV) the current peaks were lower and their maxima were recorded after longer periods (>3 s).

Experiments with TOH solutions revealed higher current densities than those recorded for Carv with current maxima that reached more than 18 mAcm^{-2} for 460 mV and 550 mV (Fig. 1B). Afterwards, current densities decrease sharply in case of 460 mV curve but maintain high values (>1 mAcm^{-2}) during the first 60 s for the other potentials. Again, marked differences can be noticed when the potentiostatic electrochemical responses of copper in Carv and TOH solutions are compared. Note that after 20 min (Fig. 1A and B insets) current density values are less than 5 μAcm^{-2} for all the potentials in case of Carv while they were higher than 200 μAcm^{-2} for TOH, 200 mV, 250 mV and 300 mV. This indicates that, unlike polyCarv, polyTOH layer is poorly protective and consequently, the position of the OH in the molecule plays an important role in the polymerization process.

Naked eye observations of polyCarv and polyTOH layers revealed that they were notoriously dissimilar since an opaque brownish layer was formed in case of polyTOH, very different from the transparent one formed with Carv (Fig. S2, Supplementary information).

3.2. FTIR spectroscopy of polyCarv and polyTOH

When FTIR spectra of polyCarv and polyTOH (Fig. 2A and B) are compared it can be noticed that there are contributions common to both spectra. However, some of the signals only appear in one of them demonstrating the importance of the selection of a particular molecular structure as it will discussed in the following section. Besides, some of these peaks can be observed exclusively in one of the potentials assayed indicating the important role of the potential in the electropolymerization process that justified the selection of a potentiostatic method better than the potentiodynamic one. Interestingly, it could also be detected that some of these contributions increase with time while others remain constant showing that the correct selection of the potentiostatic period is crucial in some cases.
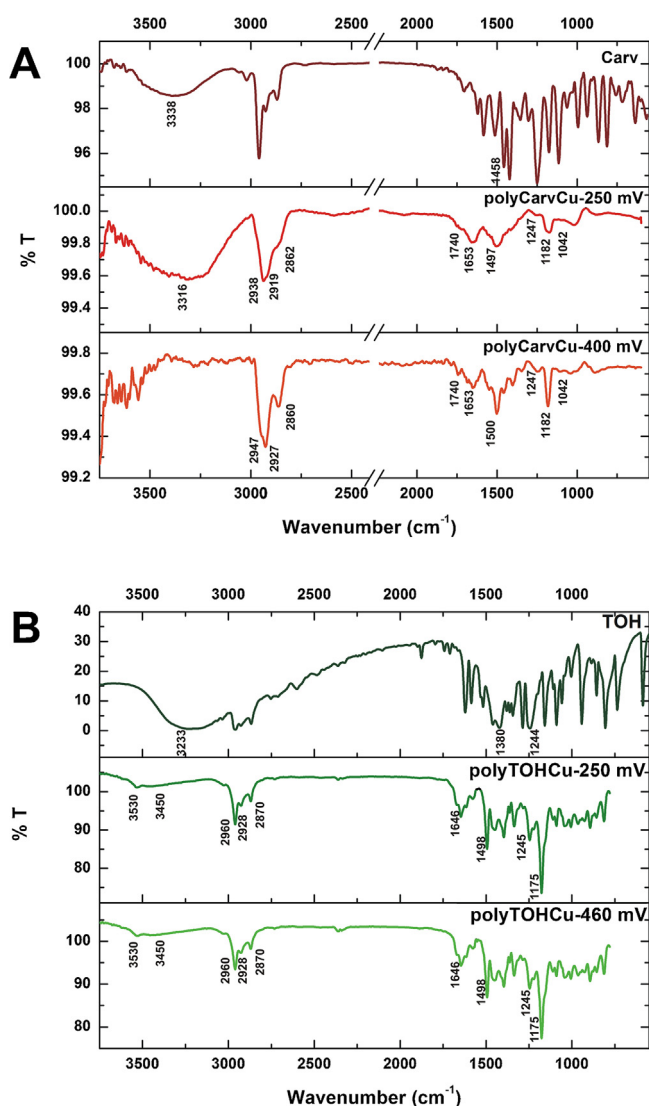
Fig. 2. A) FTIR-ATR spectra of Carv (pure drug), polyCarvCu-250 mV and polyCarvCu-400 mV, B) TOH (pure drug) and polyTOHCu-250 mV and polyTOHCu-460 mV after 20 min polymerization period.

3.2.1. Contributions present in polyTOH and polyCarv spectra

Table 1 shows contributions close to 890 cm^{-1}, 1346 cm^{-1}, 1402 cm^{-1}, 1497 cm^{-1}, 2860 cm^{-1}; 2927 cm^{-1} and 2947 cm^{-1}, that are common to all the spectra of Fig. 2 and are attributed to stretching vibrations of phenyl rings such as ν =C—H; ν_s isopropyl; 1, 2, 4 three substituted phenyl ring ν —C=C—; C=C stretch in aromatic ring; ν_s —CH$_3$; νas —CH$_2$; ν_{as} —CH$_3$, respectively, according to the references included in Table 1. They are characteristics of phenolic compounds. Additionally, those signals depicted at 1175 cm^{-1}, 1247 cm^{-1} and 1653 cm^{-1} assigned to vibration of O-containing bonds (ν C—O—C and C—O—C p-sustituted phenol; ν C—O—C; and ν —C=O, respectively) indicate the oxidation of OH groups and the formation of dimmers and oligomers with ketone and ether bonds.

Interestingly, there are contributions such as 926 cm^{-1} assigned to diphenyl ketone and that at 1006 cm^{-1} related to aliphatic —OH that are present in all the spectra except for polyCarv–250 mV.

3.2.2. Contributions present exclusively in polyCarv spectra

The peak at 1550 cm^{-1} assigned to phenyl ring ν —C=C— is shown in both, polyCarv–250 mV and polyCarv-400 mV (Table 1) but it is absent in polyTOH spectra. The band at 3316 cm^{-1} and the peak at 1020 cm^{-1} (Fig. 2A, Table 1), corresponding to ν—OH of

polyphenol formaldehyde and phenolic —C—OH, respectively, are exclusively present in polyCarv-250 mV. A similar broad band centered at 3288 cm^{-1} (close to 3316 cm^{-1} band) was previously detected for Carv adsorbed on Cu [30], and was assigned to polymeric adsorption by Kirsch and Coffin [31] that may be a previous step to the formation of electropolymerized layer. The adsorbed Carv molecules are probably at the interfacial region and form hydrogen bonds at low potentials (250 mV). However, in case of polyCarvCu-400 mV and for polyTOH-250 mV and polyTOH-460 mV this broad contribution is absent. Single adsorbed molecules were probably removed and or arranged during the fast formation of polyCarvCu-400 mV permitting the development of a highly protective compact layer.

3.2.3. Contributions present exclusively in polyTOH spectra

PolyTOH-250 mV and polyTOH-400 mV spectra show several signals that are absent in polyCarv spectra. Two of the main bands correspond to ν-OH (No H bonded, 3530 cm^{-1}) and ν-OH (H bonded, 3450 cm^{-1}) (Fig. 2B). As previously reported [23], the peak at 3530 cm^{-1} is also known as HyF/ν-OH because some authors believe that this OH cannot form H bridges with other molecules such as those of solvent, other TOH molecules, etc. It should be taken into account that TOH depicts an isopropyl group in the ortho position, relative to OH, that may obstruct the formation of H bridges with the same molecules or with the solvent. Thus, the signal may be related to the presence of TOH molecules, dimmers or oligomers confined within the polymeric matrix with OH unable to form H bridges. Another possibility is to assign this contribution to water occluded in the polymeric layer [4,10,32].

The signals at 3028 cm^{-1} and at 1614 cm^{-1} are also exclusive of polyTOH spectra (Fig. 2B) and are assigned to poly-substituted phenyl ring ν =CH (3028 cm^{-1}) and to p-substituted aromatic, 1,2,4 three substituted phenyl ring ν —C=C- and 2,4,6 trihydroxymethyl phenyl ring ν —C=C— (1614 cm^{-1}) (Table 1). Other peaks restricted to polyTOH are associated to different bonds between C and H such as aromatic ring ν —C=C— at 1464 cm^{-1}; phenyl ring ρ =C—H at 1155 cm^{-1} and ν —C=C— at 1576 cm^{-1}. On the other hand, according to the references of Table 1, those assigned to O-containing bonds are C=O Not H bonded at 1670 cm^{-1}; C—O—C aliphatic phenol-formaldehyde at 1110 cm^{-1}; ν —C—O at 1045 cm^{-1} and C—O—C stretching at 1034 cm^{-1} are characteristic of TOH oxidation and polymerization. Consequently, contributions associated only to Carv or only to TOH reveal that there are distinctive signals that characterize the oxidation and polymerization of each isomer. Thus, due to their different molecular structure and steric problems electrooxidation do not lead to similar polymeric coatings.

3.2.4. Changes of signals with time

PolyCarv and polyTOH spectra obtained after different periods reveal the strong intensification of the contributions at 1498 cm^{-1} (—C=C— of phenolic ring), and both, 1182 cm^{-1} and 1245 cm^{-1} attributed to ether bonds (Table 1) with time (Fig. 3). Thus, the increase in the number of ether bonds is related to the progression of the polymerization process. Additional increase with time was observed for 1463 cm^{-1} (—C=C— aromatic ring), at 1344 cm^{-1} (isopropyl structures) and 1245 cm^{-1} (ether bonds). This indicates that the correct selection of the potentiostatic period is crucial.

However, the signals characteristics to ketonic structures (1740 cm^{-1}, 1653 cm^{-1} and 928 cm^{-1}) did not change with time. Unlike ether bonds, ketonic structures are not associated to the polymerization progress.

Changes in polyCarv spectra with time (Fig. 3A) reveal that the band assigned to ν-OH (3000–3600 cm^{-1}), present in the spectrum of the absorbed Carv [16], almost disappeared after 1 s potentiostatization period. After this short interval the signals corresponding to ketonic structures (1740 cm^{-1}, 1648 cm^{-1} and 928 cm^{-1}), those

Table 1
Wavenumbers and assignments (according to literature data) for polyTOHCu and polyCarvCu spectra obtained at different potentials after 20 min.

Assignments	Observed wavenumber (cm⁻¹) (Fig. 2)				Literature data of wavenumber (cm⁻¹)
	polyTOH		polyCarv		
	250 mV	460 mV	250 mV	400 mV	
ν —OH (Not H bonded)	3530	3530	–	–	3522 [56]; 3535 [57]; 3525 [58,59]; 3524 [60]
ν —OH (H bonded) [56,58–60]; ν —OH···C=O [57]	3450	3450	–	–	3361 [56]; 3448–3460 [57–59]; 3366 [60]
ν-OH polyphenol-formaldehyde	–	–	3316	–	Broad band at 3389 [61]
Poly substituted phenyl ring ν=CH	3028	3028	–	–	3030 [61–63]
ν_{as} —CH3	2962	2962	2938	2947	2962 [64]; 2966 [65]
ν_{as} —CH2	2928	2926	2916	2927	2922-2940 [64]
ν_{s} —CH3	2869	2869	2862	2860	2872 [64]; 2871 [65]
—C=O Not H bonded	–	–	1740	1740	1749 [65]
—C=O Not H bonded	1670	1668	–	–	1680 [58]
ν —C=O [58,66–69]; ν —C=C— [70]	1646	1647	1653	1653	1654 [58]; 1653 [66]; 1641 [70]; 1648 [67]; 1640–1660 [68,69]
Polysubstituted phenyl ring ν —C=C—^{a}	1614	1614	–	–	1612 [65]; 1610 [61,66]
ν —C=C—	1576	1576	–	–	1575 [62]
Phenyl ring ν —C=C—	–	–	1547	1550	1552 [61]; 1540–1560 [66]
Phenyl ring ν C=C	–	–	1512	1511	1513 [61]; 1498–1514 [71]
C=C stretch in aromatic ring	1498	1498	1497	1500	1497 [64]; 1470 [72]; 1492 [67]
Aromatic ring ν —C=C—	1464	1461	–	1465	1466 [64]; 1470 [72]; 1461 [73]
ν_{as} isopropyl	1447	1447	–	1459	1430-1485 [62]
1,2, 4 three substituted phenyl ring ν —C=C—	1397	1397	1413	1402	1400 [66]
ν_{as} isopropyl	1363	1362	1363	1366	1363 [65]
ν_{s} isopropyl	1337	1337	1348	1346	1350-1380 [74]
ν C—O—C	1245	1245	1252	1247	1247 [74]
Phenyl ring ρ =C—H	1223	1221	–	–	1215 [66]
ν C—O—C [66,67,72,74]; ν C—O—C p-sustituted phenol [65]	1175	1175	1182	1182	1178 [65]; 1190 [66,67]; 1188 [72]; 1184 [74]
Phenyl ring ρ =C—H [66,67]	1155	1155	–	–	1155 [66]; 1160 [67]
C—O—C aliphatic phenol-formaldehyde	1110	1110	–	–	1116 [61]
ν —C—O	1045	1045	–	–	1058 [61]; 1046 [64]
C—O—C stretching	1034	1034	–	–	1036 [74]
Phenyl —C—OH	–	–	1020	–	1023 [61]
Aliphatic —OH [61]; Phenyl ring ρ =C—H [66]	1006	1006	–	1002	1000-1010 [61]; 1010 [66]
Diphenyl Ketone	926	926	–	929	925 [66]
phenyl ring ν =C—H	894	894	879	890	892 [71]

ν_{as} = asymmetrical stretching vibration.
ν_{s} = symmetrical stretching vibration.
ρ = in plane vibration.
^{a} = p-substituted aromatic [65]; 1,2, 4 three substituted phenyl ring ν —C=C— [66]; 2,4,6 trihydroxymethyl phenyl ring ν —C=C— [61].

at 1455 cm⁻¹ and 1181 cm⁻¹ attributed to ether unions, 1465 cm⁻¹, 1514 cm⁻¹ and 1542 cm⁻¹ associated to phenyl ring ν —C=C can be visualized. Other assigned to isopropyl structures (1344 cm⁻¹ and 1369 cm⁻¹) as well as the region 2854–2945 cm⁻¹ (ν —CH2/—CH3) can also be noticed.

In case of polyTOH after different periods (Fig. 3B) the narrow band at 3530 cm⁻¹ and the broad band at ca. 3443 cm⁻¹ increased with the potentiostatic period together with a strong intensification in 2960–2870 cm⁻¹ band, revealing changes in the composition of the layer with time probably due to the accumulation of TOH single molecules, dimmer, oligomers and/or water that remain in the surrounding region. Additionally the increase of almost all the contributions in the 1576–1006 cm⁻¹ region was noticed. These results show the changes of the composition of the layer over time.

Assuming that some molecules may be confined within the polymeric layers or in the rifts detected in AFM images (Fig. S3, Supplementary information), it may be hypothesized that the amount of these molecules increases with time. In fact, the width of the rifts increases with time. Anyhow, this complex polyTOH structure is probably related to the oxidation current that remains high in case of polyTOH but not in case of polyCarv.

3.3. AFM analysis

AFM analysis provided interesting information about the roughness and thickness of the polymeric films and size of the round nanoflakes formed on the Cu surface. Comparisons of the coatings potentiostatically obtained at the potential of the peaks recorded during the cyclic polarization (400 mV for Carv and 460 mV for TOH, Fig. S1) and at a lower potential (250 mV) after identical periods (20 min) were made in Fig. 4.

PolyCarv films obtained after 20 min of polarization at 250 mV and 400 mV (Fig. 4) are bright and smooth and show that the roughness is lower in case of polyCarv-400 mV with smaller nanofeatures (Ra = 1.6 nm and Rq = 2.3 nm) than those obtained at lower potentials (polyCarv-250 mV, Ra = 2.6 nm and Rq = 3.3 nm). On the other hand, those attained with polyTOH (Fig. S4-A, Fig. S4-B, Supplementary information) are opaque and depicted higher roughness parameters. However, unlike Carv layers, polyTOH layers show higher Ra, Rq and Rmax at higher potentials (Ra = 4.1 nm for 250 mV, Fig. S4-A; Ra = 8.4 nm for 460 mV, Fig. S4-B).

Interestingly, after 1 s of potentiostatic polarization in a Carv solution it can be noticed that there are nanopores of different depth on the surface (Fig. S5, Supplementary information). Their
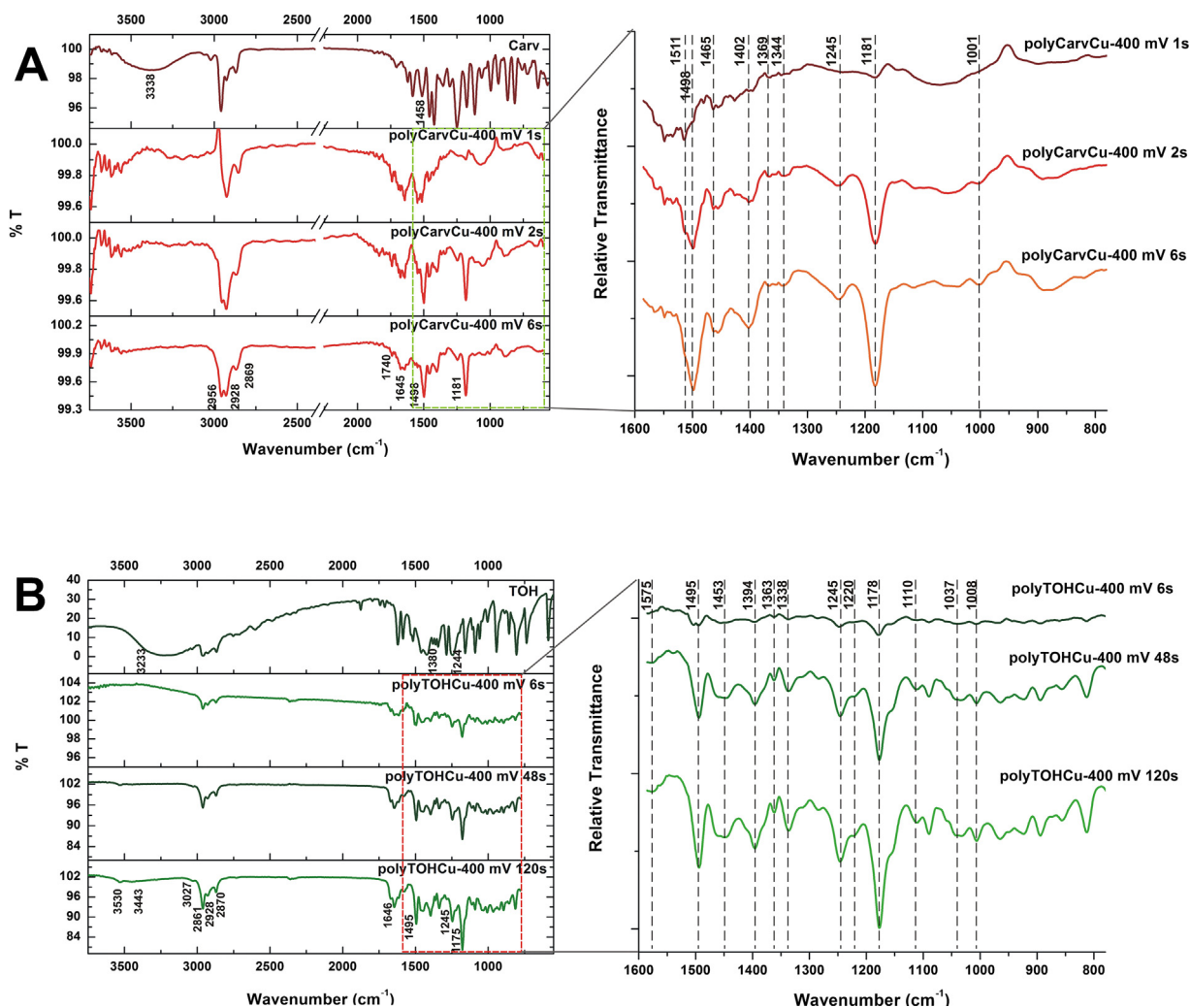
Fig. 3. FTIR-ATR spectra obtained after polarization at 400 mV during different periods (1 s, 2 s and 6 s) for Carv (A), and (6 s, 48 s and 120 s) for TOH (B).
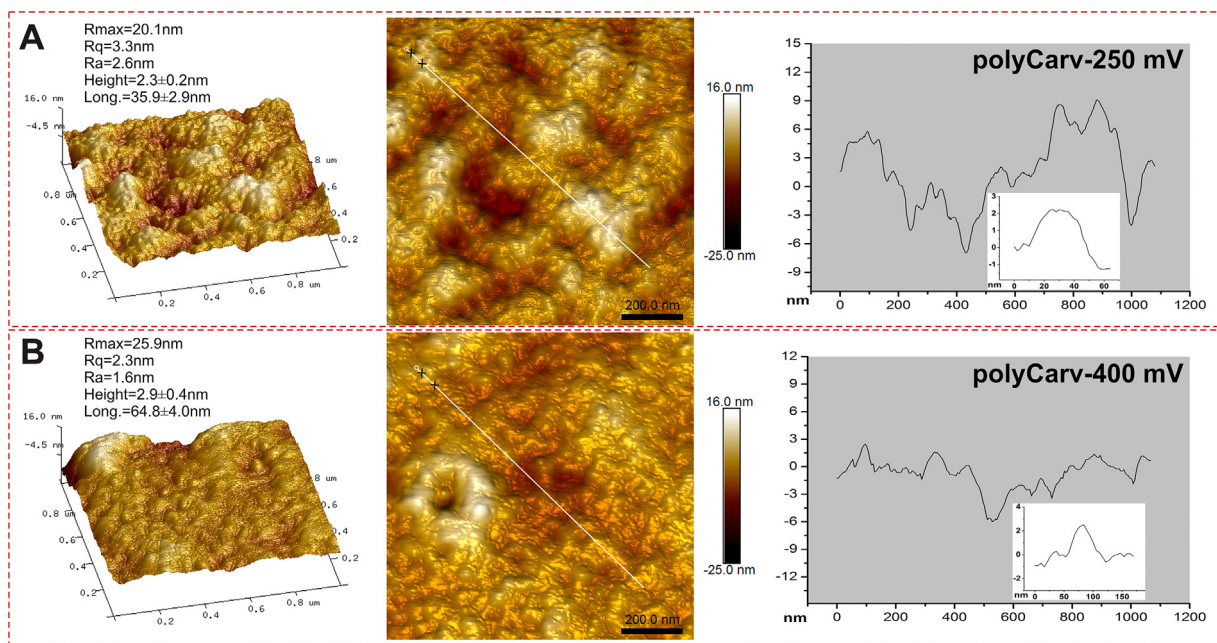

Fig. 4. AFM images of electropolymerized layers obtained after 20 min polarization in a Carv solution at 250 mV (A) and 400 mV (B). Section analyses corresponding to the white lines are shown on the right. The insets correspond to details associated to the lines between black crosses. Note that the magnification of the height (z axis) of the images of polyCarv layers is 5 times higher than that of polyTOH (Fig. S6).

Table 2
Copper ions release after 6 days of exposure of copper samples with and without Carv or TOH potentiostatic (200 mV- 550 mV potential range) and potentiodynamic (1 cycle and 39 cycles) electropolymerization treatments. (Mean values ± standard error of the mean; n = 3).

Carv		TOH	
Treatment	$[Cu^{2+}]$ ($\mu g\,cm^{-2}$)	Treatment	$[Cu^{2+}]$ ($\mu g\,cm^{-2}$)
Potentiostatic treatment			
200 mV	8.46 ± 1.90		
250 mV	5.12 ± 0.54	250 mV	39.75 ± 5.41
400 mV	4.74 ± 1.51	400 mV	23.83 ± 4.07
		460 mV	20.35 ± 5.08
		550 mV	23.03 ± 0.12
Potentiodynamic treatment			
1 cycle	33.22 ± 7.59	1 cycle	45.86 ± 2.40
39 cycles	14.64 ± 0.88	39 cycles	31.45 ± 3.17
Bare Cu			
Without treatment	132.36 ± 29.03		

diameters seem to decrease with time because lower numbers of pores were found after longer potentiotatization periods until a smooth layer is formed (Fig. 4B).

The analysis of the different stages of the electroformation of polyTOH layers (Fig. S6) revealed that after 6 s the metal surface was covered by large globular features (89.4 ± 4.5 nm diameter) that formed a polymeric film with Ra = 10.1 nm and Rq = 12.8 nm. After 48 s the roughness increases drastically (Ra = 17.2 nm and Rq = 21.7 nm) due to the accumulation of new globular features on the old ones. The layer became thicker after 120 s with little changes in roughness values but, after 20 min, it developed into a more compact coating (Fig. S6). It is worth mentioning that the layers are not uniform and regions of different thickness can be distinguished on the polyTOHCu surface (Fig. S3) similar to that described previously for other phenolic compounds [33]. This information confirms the importance of the proper selection of the polymerization time to optimize the characteristics of the layers.

3.4. Copper ions release in the presence and in the absence of the electropolymerized layers

Measurements of copper ions released by copper discs, with and without the potentiostatic electropolymerization treatments, immersed in 0.136 M KCl solution are shown in Table 2. After 6 days of immersion, the content of copper in the chloride solution in case of bare copper reaches 132.36 ± 29.03 $\mu g\,cm^{-2}$ while the best protective performance was achieved by polyCarvCu (after 20 min at 0.4 V) with 4.74 ± 1.51 $\mu g\,cm^{-2}$. Concentration values of copper released by polyTOHCu (23.83 ± 4.07 for 0.4 V) were four times higher than those of polyCarvCu in agreement with the electrochemical response that showed higher current values for TOH. Again, results show that Carv treatments are more effective than those of TOH. They also show that a better performance is obtained by potentiostatic technique than by cyclic potentiodynamic treatment (1 cycle and 39 cycles, Table 2).

3.5. Evaluation of transient currents using nucleation and growth model

Considering the electrochemical and surface analysis it seems that a suitable model to interpret the mechanism involved in the formation of the layers is the nucleation and growth model. It was adapted from Garfias-García et al. [34] and involves the reactions previously reported [23]. These authors applied Bewick, Fleischmann and Thrisk theory to analyse the chronoamperometric results [35–37] with successfully outcome in case of pyrrole.

As it can be seen in Fig. 1 the transient currents obtained for polyCarvCu–400 mV and polyTOHCu–460 mV showed that the time needed to reach a stationary state is longer and current values are higher in case of TOH, this variation is probably associated to different growth mechanisms for these polymeric layers. Thus, the electrochemical response is dependent on the selection of the fixed potential and on the monomer used (Carv or TOH).

In view of the current transient fittings it seems that in case of Carv, at potentials in the 0.3 V–0.5 V, only heterogeneous reactions at the electrode–solution interface are mainly involved [23] leading to 2D growth. At potentials near 400 mV it seems that the adsorbed molecules and oligomers can be quickly assembled into an ordered layer resulting in very compact and highly protective transparent polyCarv film (Fig. 5) that inhibits further oxidation.

In case of TOH, some molecules may form dimmers and oligomers that probably react later with the adsorbed molecules and develop aggregates or remain in the surrounding aqueous environment leading to the non-homogeneous layer detected by AFM (Fig. S6, Fig. S4, Supplementary information). The different growth mechanisms of polyCarv and polyTOH may be related to the molecular structures of the isomers. According to its chemical structure, OH group of TOH is close to the isopropyl group and the formation of an ordered adsorbed layer may be hindered due to steric impediments. In fact, higher roughness was found on polyTOH surface by AFM (Fig. S4) and cauliflower-like deposits were detected [38]. The soft loosely adherent polyTOH layer may allow the electrical transport needed to oxidize new soluble species. This is consistent with the 3D growth suggested for the current transient fittings.

Thus, in case of Carv 200 mV, 400 mV and TOH 460 mV we proposed that the overall rate of the electrodic process (Jtot(t)) is given by the sum of three contributions according to Eq. (1) (a more detailed description is provided as Supplementary Information):

$$Jtot(t) = Joxi(t) + J2Di(t) + J2Dp(t) \tag{1}$$

Joxi(t) = due to the phenolic compound oxidation on copper surface to form oxidized molecules and different dimmers and oligomers adsorbed at the surface.

J2Di(t) = related to the instantaneous bidimensional nucleation of the adsorbed molecules and oligomers.

J2Dp(t) = assigned to the two dimensional progressive nucleation of phenolic species

In case of polyTOH the use of a J3Di(t) component related to the instantaneous three dimensional nucleation (instead of J2Dp(t)) was necessary to fit the transient currents for potentials lower than 460 mV according to Eq. (2).

$$Jtot(t) = Joxi(t) + J2Di(t) + J3Di(t) \tag{2}$$

J3Di(t) is the main contribution of polyTOH-200 mV after the first 20 s. This contribution is absent in the polyTOH-460 mV fitting processes and may be related to the heterogeneous characteristics of the TOH layers with 3D structures mainly formed at potentials other than 460 mV (Fig. S7). At these potentials current densities remain high and decrease slowly after the first 10 s (Fig. 1). Thus, this heterogeneous 3D layer is less protective than polyCarv coating. Importantly, a similar fitting with J2Di(t) and J3Di(t) was found in case of pyrrole electropolymerization in the presence of hexafluorates [39].

The fitting process was helpful to interpret the process that justified the selection of the more proper isomer (Carv) and better conditions (400 mV, >30s) to obtain 2D components with the higher maxima after short periods that provide the best protective characteristics.
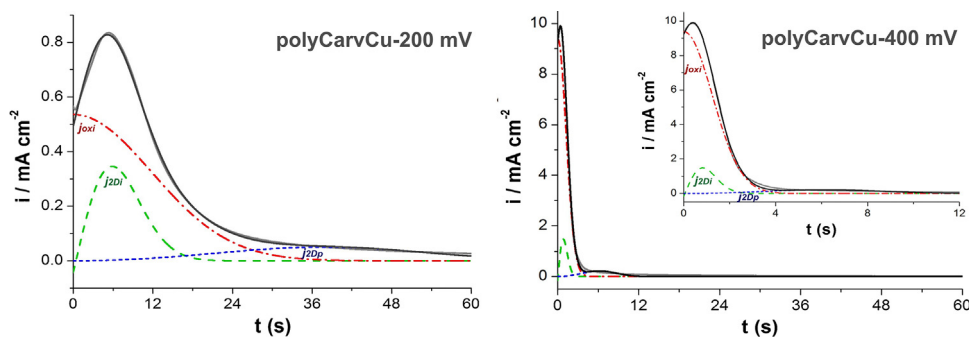
Fig. 5. (– –) Chronoamperometric records obtained during the electropolymerization of Carv at 400 mV and 200 mV. (—)Theoretical transients obtained by a nonlinear fitting of experimental data using Eq. (1) (The individual contributions to the overall current, Joxi(t), J2Di(t) and J2Dp(t) are also shown).

3.6. Comparative analysis of the characteristics of the different polymeric layers

In view of the copper release measurements and AFM images, oxidation of copper seems to occur at the sites covered by thin and non compact layers that operate like pores and rifts. They contribute to the total current, being more important for polyTOH than for polyCarv.

Considering ATR-FTIR results that revealed the presence of v-OH and the low current values recorded in case of polyCarv 250 mV, it can be hypothesized that at low potentials (<300 mV) Carv molecules adsorb on the copper surface, but only some molecules are oxidized and remain attached on the surface. At higher potentials (400 mV) the molecules can be firstly ordered with their OH group facing the metal [40] with the aromatic ring pointed toward the bulk of the solution. In a second step the molecule may be reoriented parallel to the electrode surface [41,42]. Due to the radical instability at "ortho" and "para" positions polymerization occurs in this positions. The presence and position of substituents on the phenolic ring frequently determine the rate of electropolymerization, the intermediate phenoxyl radicals and reaction products and how they will be adsorbed at the electrode [40].

This probably favours the oxidation and polymerization processes leading to the formation of a compact layer that quickly blocked the metal surface and hinders oxidation and corrosion with the consequent abrupt decrease in the current density.

In case of TOH, owing to the presence of OH close to the isopropyl group, the formation of an ordered adsorbed layer is probably more impeded than in case of Carv leading to a non homogeneous polymerization. When ATR-FTIR, AFM and chronoamperometric results are jointly analyzed it may be inferred that the high current values recorded after the first 10 s are probably related to the oxidation of TOH leading to the formation of dimmers and oligomers that later precipitate on the previously formed layers. Thus, a loosely protective structure generated by the non homogeneous layers with 3D features that are formed or deposited on the surface is developed. Interestingly, chronoamperometric measurements and AFM images show that a more compact structure is formed at the peak potential (460 mV) with suitable conditions to develop a more ordered and protective layer than at other potentials. Unlike Carv, TOH polymerization at potentials other than 460 mV leads to higher current values that remain elevated after 10 s (Fig. 1). Therefore, oxidation seems to be favored on this heterogeneous structure leading to higher quantities of ether and quinones groups detected by IR spectroscopy. In view of the high copper ions release from polyTOHCu in KCl solutions after 6 days under open circuit potential condition, the oxidation rate of copper in the less protective sites of the heterogeneous polyTOH layer is more significant than in case of polyCarv.

3.7. Biological assays: clonogenic test

Clonogenic assays show the differences in reproductive viability, i.e. capacity a single cell to form a colony of 50 or more cells, between control untreated cells and cells that have been exposed to a particular treatment. Results showed a drastic decrease (>99%) in the number of MC3T3-E1 colonies with respect to the control in case of pure Cu without treatment, confirming the strong cytotoxic effect of these metal ions. Lower cytotoxicity than bare Cu was attained in case of polyTOHCu, revealing a reduction in the number of colonies to ca. 30% (polyTOHCu-460 mV) and ca. 44% (polyTOHCu-250 mV) of the control value (without metal disc). These values are closely related with the concentration values of the released copper. A better performance was found in case of polyCarvCu, with minimal variation with respect to the control for polyCarvCu-400 mV (ca. 96%) while ca. 82% was found for polyCarvCu-250 mV. Again, these results can be associated to the low values of copper ions release. A similar tendency was found in the analysis of the diameters of the colonies.

It is worth mentioning that the toxic effect is distance-dependent (i.e. copper concentration dependent) in case of TOH treatment [43]. Thus, colonies formed further than 18 mm (region B) in presence of polyTOHCu showed better growth than those of region A, after either the treatments at 250 mV or 460 mV (Fig. 6A). On the other hand, there are significant differences between polyCarvCu-400 mV and polyTOHCu-460 mV and between polyCarvCu-250 mV and polyTOHCu-250 mV showing that Carv treatments are more efficient and lead to more biocompatible condition than TOH treatments.

In region A, close to the metal sample, where the concentration of release copper is higher [43], colonies formed in the presence of polyTOHCu were markedly smaller (p ≤ 0.001) than those formed in presence of polyCarvCu (Fig. 6A and B). No significant difference in relation to the control was observed for polyCarvCu–400 mV but the change was low but significant in case of polyCarvCu-250 mV (p ≤ 0.001). Thus, the treatment with Carv at 400 mV proved to be the most favorable condition with the stronger protective effect, evidenced by the lowest copper ions release and a colony formation similar to the control in number and diameter, after 6 days of incubation.

It has been reported that the medical industry has focused research dollars into copper and its alloys. It can be effectively used to carry signals to small implants and diagnostic tools. Due to its high conductivity, it is possible to replace larger or more expensive materials by smaller copper wires into devices which are able to send and receive signals or carry electrical charges needed for the proper operation of the device [44]. Limits to its thrombogenic risks have been accurately overcome by shielded copper. Polymeric coatings such as polyCarv could be used as an appropriate biocompatible method to protect copper surface. Another medical
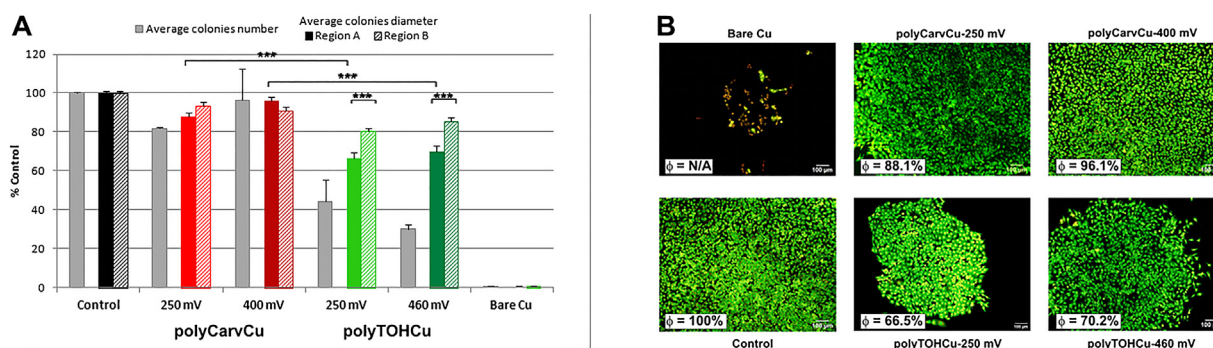
Fig. 6. A) (grey bar) Average number of MC3T3-E1 colonies formed in the absence (control) and in the presence of coatings (polyCarvCu and polyTOHCu) (error bars indicate standard error of the mean obtained on independent three experiments). Average diameter (ϕ) of MC3T3-E1 colonies grown in region A (area close to the metal, filled coloured bars) and B (far from the metal, striped bars) in the absence (control) and the presence of polyCarvCu (250 mV and 400 mV), polyTOHCu (250 mV and 460 mV) and bare Cu discs (brown bar) after 6 days of exposure (error bars indicate standard error of the mean; n = 60). (*** Significance of the difference at p ≤ 0.001). B) Photomicrographs of 6 days colonies grown in the presence of bare Cu, polyCarvCu (250 mV and 400 mV) or polyTOHCu (250 mv and 460 mV) treatments. Average diameter (ϕ = % of the control) is included in each picture. Magnification: 100×.

application of copper wires is related to the intrauterine devices (IUD) that are inserted in the uterus for contraception. Thin layers of polyCarv could control the release of copper ions avoiding the undesirable effects of burst release [45,46]. *In vitro* assays to test biocompatibility reported here have been useful to disregard toxic effects of the compound on mammalian cells and also to evaluate the possibility of the use of the polyCarv in medical devices.

3.8. Comparison of conventional corrosion inhibition treatments with eco-friendly polyCarv

At this point it is important to analyse which the benefits of the eco-friendly corrosion inhibition treatment proposed here in relation to conventional treatments are. Considering exclusively the damage of tubes, equipments and/or devices that suffer degradation, research has been generally focused on the development of a compound/coating able to achieve the better inhibition performance [47]. However, it is important to bear in mind that the impact of corrosion is not limited to this devastation. Corrosion is also a form of waste that leads to environmental pollution by metal ions release.

In case of copper corrosion, higher inhibition efficiency is often achieved by application of organic compounds related to inorganic. Amines, thiazoles, benzotriazoles, triazoles and derivatives offer good protection. The selection is generally made considering profitable criteria. Some of them, like amines, show good inhibition and they are not expensive but their application in the systems is not economically acceptable because high concentration is needed in the water that is in contact with the metal while others are unacceptable due to their high price [47]. Excluding the analysis of environmental impact, the use of organic corrosion inhibitors that are added to the water still remains to be one of the most economically viable methods. This is due to their easy application through batch and/or continuous treatments with small amounts of material. However the economical analysis of corrosion control should not be restricted to the evaluation of the cost of corrosion prevention and the benefits of the reduction of metal ions release to the environment. It must consider that corrosion control creates other source of contamination that should be eliminated: the release of toxic corrosion inhibitors that may hazardously impact on the surroundings. For example, benzothiazoles and benzotriazoles are highly efficient as copper corrosion inhibitors [48–51] but they show limited removal from wastewater by conventional treatments and have been classified as emerging organic pollutants. Due to the similarity of the benzothiazole molecular structure with purines these compounds may interact with biomolecules and

trigger the risk for the biological media. On the other hand, benzotriazoles are stable to heat, ultraviolet radiation and chemical or bacterial attack but these characteristics makes them persistent xenobiotics under environmental conditions. They have also been identified as carcinogenic substances and have been shown to induce toxic responses in fish, invertebrates and marine and soil bacteria at low concentrations [52,53]. As compared to these organic inhibitors, polymeric materials are not yet as widely used. Conventional polymer coatings provide corrosion protection by acting as a barrier layer between the substrate material and the environment, however, some of them are permeable to water, gas and/or ions depending on the characteristics of the polymer coating and the technique of the coating application. However, if they penetrate through the coating and reach the substrate, corrosion reactions occur at the metal/coating interface and can cause damage to the coating [54]. It is important to highlight that another disadvantage of synthetic coatings is their capacity to change cellular interactions and modify copper mechanism of toxicity. These findings have significant implications for the evaluation of toxicological risks of these coatings associated to a higher generation of reactive oxygen species (ROS) [55].

All things considered, the electroformation of polyCarv for Cu corrosion inhibition emerges as a novel natural, and sustainable alternative to be pondered. It is also cost-effective since the price of essential oils is similar to those of the organic inhibitors but the amount used is very low since they are used to form the coating and should not be added to the water and no supplementary cost to eliminate toxic contaminants that come from the release of the inhibitor should be taken into account. Furthermore, very important considering the environmental impact (although it is difficult to be weighed), good biocompatibility was demonstrated for the polyCarv-Cu and very low PEI and carbon footprint are related to its production which demonstrate its minimal damage to the biological media.

4. Summary and conclusions

Results highlight the importance of the detailed study of the evolution of the electropolymerization processes of phenolic compounds as a previous step for the selection of the best biocompatible condition, due the high impact of molecular structure, potential perturbation and polarization time on the characteristics of the resulting polymeric layers. According to the selected compound and electrochemical perturbation, films of particular composition, structure, protective properties and biocompatibility are attained.

The electrochemical, AFM and spectroscopic results as well as copper ions release measurements reveal that the potentiostatic electropolymerization treatment is more efficient than the potentiodynamic one. Additionally, they show that the evolutions of the potestiostatic polymerization processes of Carv and TOH are different. According to ATR-FTIR analysis, Carv and TOH oxidation occurs during potentiostatic treatments and dimmers, oligomers and polymeric layers are progressively formed, at higher rate in case of Carv. The composition and structure of the layers depend on the phenolic compound and change with potential and polarization time. Polymeric layers include the formation of ether bonds that increases with time and are more homogeneous and protective, and less rough in case of polyCarvCu. PolyTOHCu include rifts and pores that remain after the treatment and probably facilitate the access of the phenolic molecules and aggressive ions to the active sites of the metal surface favoring the oxidation of copper and single organic molecules.

Simulations of current transients using the nucleation and growth model reveal different contributions that include the electroadsorption process and 2D instantaneous and progressive nucleation in case of polyCarv, while 3D nucleation is an additional component needed to fit the current transient in case of the poly-TOH layer and justifies the heterogeneous characteristics of this film.

Protective polyCarv ecofriendly coatings that can be obtained by the electropolymerization of phytocompounds impact beneficially on the environment due to the reduction of Cu ions release from copper-based materials. The appropriate selection of the potential is crucial to obtain the best biocompatible condition.

Acknowledgements

Appendix A. Supplementary data

Supplementary data associated with this article can be found, in the online version, at http://dx.doi.org/10.1016/j.colsurfb.2017.08.029.

References

[1] S.H. Lee, J.G. Kim, J.Y. Koo, Investigation of pitting corrosion of a copper tube in a heating system, Eng. Fail. Anal. 17 (2010) 1424–1435, http://dx.doi.org/10.1016/j.engfailanal.2010.05.002.

[2] H. Bi, G.T. Burstein, B.B. Rodriguez, G. Kawaley, Some aspects of the role of inhibitors in the corrosion of copper in tap water as observed by cyclic voltammetry, Corros. Sci. 102 (2016) 510–516, http://dx.doi.org/10.1016/j.corsci.2015.11.005.

[3] R.E. Melchers, Bi-modal trends in the long-term corrosion of copper and high copper alloys, Corros. Sci. 95 (2015) 51–61, http://dx.doi.org/10.1016/j.corsci.2015.02.001.

[4] A. Drach, I. Tsukrov, J. DeCew, J. Aufrecht, A. Grohbauer, U. Hofmann, Field studies of corrosion behaviour of copper alloys in natural seawater, Corros. Sci. 76 (2013) 453–464, http://dx.doi.org/10.1016/j.corsci.2013.07.019.

[5] X. Zhang, I.O. Wallinder, C. Leygraf, Mechanistic studies of corrosion product flaking on copper and copper-based alloys in marine environments, Corros. Sci. 85 (2014) 15–25, http://dx.doi.org/10.1016/j.corsci.2014.03.028.

[6] G. Kear, B.D. Barker, F.C. Walsh, Electrochemical corrosion of unalloyed copper in chloride media–a critical review, Corros. Sci. 46 (2004) 109–135, http://dx.doi.org/10.1016/s0010-938x(02)00257-3.

[7] S. Khan, A.A. Ansari, A.A. Khan, M. Abdulla, O. Al-Obaid, R. Ahmad, In vitro evaluation of cytotoxicity, possible alteration of apoptotic regulatory proteins, and antibacterial activity of synthesized copper oxide nanoparticles, Colloids Surf. B Biointerfaces 153 (2017) 320–326, http://dx.doi.org/10.1016/j.colsurfb.2017.03.005.

[8] J. Hedberg, H.L. Karlsson, Y. Hedberg, E. Blomberg, I. Odnevall Wallinder, The importance of extracellular speciation and corrosion of copper nanoparticles

on lung cell membrane integrity, Colloids Surf. B Biointerfaces 141 (2016) 291–300, http://dx.doi.org/10.1016/j.colsurfb.2016.01.052.

[9] B.R. Lewandowski, D.A. Lytle, J.C. Garno, Nanoscale investigation of the impact of pH and orthophosphate on the corrosion of copper surfaces in water, Langmuir 26 (2010) 14671–14679, http://dx.doi.org/10.1021/la102624n.

[10] I. Vopálenská, Z. Palková, L. Váchová, Z. Palková, New biosensor for detection of copper ions in water based on immobilized genetically modified yeast cells, Biosens. Bioelectron. 72 (2015) 160–167, http://dx.doi.org/10.1016/j.bios.2015.05.006.

[11] E. Abelev, D. Starosvetsky, Y. Ein-eli, Enhanced Copper Surface Protection in Aqueous Solutions Containing Short-Chain Alkanoic Acid Potassium Salts, Langmuir 23 (2007) 11281–11288.

[12] M. Schwind, S. Hosseinpour, C.M. Johnson, C. Langhammer, I. Zoric, C. Leygraf, et al., Combined in situ quartz crystal microbalance with dissipation monitoring, indirect nanoplasmonic sensing, and vibrational sum frequency spectroscopic monitoring of alkanethiol-protected copper corrosion, Langmuir 29 (2013) 7151–7161.

[13] Z. Khiati, A.A. Othman, M. Sanchez-Moreno, M.C. Bernard, S. Joiret, E.M.M. Sutter, et al., Corrosion inhibition of copper in neutral chloride media by a novel derivative of 1,2,4-triazole, Corros. Sci. 53 (2011) 3092–3099, http://dx.doi.org/10.1016/j.corsci.2011.05.042.

[14] M.A. Quraishi Sudheer, Electrochemical and theoretical investigation of triazole derivatives on corrosion inhibition behavior of copper in hydrochloric acid medium, Corros. Sci. 70 (2013) 161–169, http://dx.doi.org/10.1016/j.corsci.2013.01.025.

[15] S.M. Milić, M.M. Antonijević, Some aspects of copper corrosion in presence of benzotriazole and chloride ions, Corros. Sci. 51 (2009) 28–34, http://dx.doi.org/10.1016/j.corsci.2008.10.007.

[16] Y.C. Pan, Y. Wen, R. Zhang, Y.Y. Wang, Z.R. Zhang, H.F. Yang, Electrochemical and SERS spectroscopic investigations of 4-methyl-4H-1, 2, 4-triazole-3-thiol monolayers self-assembled on copper surface, Appl. Surf. Sci. 258 (2012) 3956–3961, http://dx.doi.org/10.1016/j.apsusc.2011.12.070.

[17] H. Tian, Y.F. Cheng, W. Li, B. Hou, Triazolyl-acylhydrazone derivatives as novel inhibitors for copper corrosion in chloride solutions, Corros. Sci. 100 (2015) 341–352, http://dx.doi.org/10.1016/j.corsci.2015.08.022.

[18] P.G. Cao, J.L. Yao, J.W. Zheng, R.A. Gu, Z.Q. Tian, Comparative study of inhibition effects of benzotriazole for metals in neutral solutions As observed with surface-Enhanced raman spectroscopy, Langmuir 18 (2002) 100–104.

[19] Z. Xu, S. Lau, P.W. Bohn, The role of nitrogen and sulfur heterocycles in corrosion inhibition. 1. Initial steps in the adsorption of benzotriazole at Copper(I) and Copper(II) oxides, Langmuir 9 (1993) 993–1000.

[20] M. Shahid, Corrosion protection with eco-friendly inhibitors, Adv. Nat. Sci. Nanosci. Nanotechnol. 2 (2011) 1–6, http://dx.doi.org/10.1088/2043-6262/2/4/043001.

[21] S. Bracke, S. Yamada, Y. Kinoshita, M. Inoue, T. Yamada, Decision making within the conceptual design phase of eco-Friendly products, Procedia Manuf. 8 (2017) 463–470, http://dx.doi.org/10.1016/j.promfg.2017.02.059.

[22] J. Moncada, J.A. Tamayo, C.A. Cardona, Techno-economic and environmental assessment of essential oil extraction from Oregano (Origanum vulgare) and Rosemary (Rosmarinus officinalis) in Colombia, J. Clean. Prod. 112 (2016) 172–181, http://dx.doi.org/10.1016/j.jclepro.2015.09.067.

[23] M. Bertuola, D. Pissinis, A. Rubert, E. Prieto, M.A. Fernández Lorenzo, Impact of molecular structure of two natural phenolic isomers on the protective characteristics of electropolymerized nanolayers formed on copper, Electrochim. Acta 215 (2016) 289–297.

[24] F. Bakkali, S. Averbeck, D. Averbeck, M. Idaomar, Biological effects of essential oils − A review, Food Chem. Toxicol. 46 (2008) 446–475, http://dx.doi.org/10.1016/j.fct.2007.09.106.

[25] A. Guenbour, A. Kacemi, A. Benbachir, L. Aries, Electropolymerization of 2-aminophenol. Electrochemical and spectroscopic studies, Prog. Org. Coatings. 38 (2000) 121–126, http://dx.doi.org/10.1016/S0300-9440(00)00085-0.

[26] A. Guenbour, A. Kacemi, A. Benbachir, Corrosion protection of copper by polyaminophenol films, Prog. Org. Coatings. 39 (2000) 151–155, http://dx.doi.org/10.1016/S0300-9440(00)00141-7.

[27] G. Mengoli, M.M. Musiani, An overview of phenol electropolymerization for metal protection, J. Electrochem. Soc. 134 (1987) 643C–652C, http://dx.doi.org/10.1149/1.2100379.

[28] M.J. Ahmed, M. Saifuddin, T. Jannat, S.C. Bhattacharjee, A rapid spectrophotometric method for the determination of copper in real, environmeental biological and soil samples using 1-(2-pyridylazo)-2-naphthol, Green Chem. 4 (2010) 1–12.

[29] N.A.P. Franken, H.M. Rodermond, J. Stap, J. Haveman, C. van Bree, Clonogenic assay of cells in vitro, Nat. Protoc. 1 (2006) 2315–2319, http://dx.doi.org/10.1038/nprot.2006.339.

[30] M. Bertuola, C.A. Grillo, M.A. Fernández Lorenzo, Reduction of copper ions release by a novel ecofriendly electropolymerized nanolayer obtained from a natural compound (carvacrol), J. Hazard. Mater. 313 (2016) 262–271, http://dx.doi.org/10.1016/j.jhazmat.2016.03.086.

[31] J.L. Kirsch, D.R. Coffin, Infrared and nuclear magnetic resonance studies of hydrogen bonding in aliphatic alcohol systems, J. Phys. Chem. 80 (1976) 2448–2451.

[32] D.A. Shifler, Understanding material interactions in marine environments to promote extended structural life, Corros. Sci. 47 (2005) 2335–2352, http://dx.doi.org/10.1016/j.corsci.2004.09.027.

[33] J. Wang, M. Jiang, F. Lu, Electrochemical quartz crystal microbalance investigation of surface fouling due to phenol oxidation, J. Electroanal. Chem. 444 (1998) 127–132.

[34] E. Garfias-García, M. Romero-Romo, M.T. Ramírez-Silva, J. Morales, M. Palomar-Pardavé, Mechanism and kinetics of the electrochemical formation of polypyrrole under forced convection conditions, J. Electroanal. Chem. 613 (2008) 67–79, http://dx.doi.org/10.1016/j.jelechem.2007.10.013.

[35] A. Bewick, B. Thomas, Optical and electrochemical studies of the under-potential deposition of metals. Part II. Phase transitions and two-dimensional nucleation, J. Electroanal. Chem. Interfacial Electrochem. 85 (1977) 329–337, http://dx.doi.org/10.1016/S0022-0728(77)80235-0.

[36] A. Bewick, M. Fleischmann, H.R. Thirsk, Kinetics of the electrocrystallization of thin films of calomel, Trans. Faraday Soc. 58 (1962) 2200, http://dx.doi.org/10.1039/tf9625802200.

[37] A. Bewick, B. Thomas, Optical and electrochemical studies of the under-potential deposition of metals Part III. Lead deposition on silver single crystals, J. Electroanal. Chem. 84 (1977) 127–140.

[38] J.I. Martins, M. Bazzaoui, T.C. Reis, S.C. Costa, M.C. Nunes, L. Martins, et al., The effect of pH on the pyrrole electropolymerization on iron in malate aqueous solutions, Prog. Org. Coat. 65 (2009) 62–70, http://dx.doi.org/10.1016/j.porgcoat.2008.09.011.

[39] M. Chmielewski, M. Grzeszczuk, J. Kalenik, A. Kpas-Suwara, Evaluation of the potential dependence of 2D-3D growth rates and structures of polypyrrole films in aqueous solutions of hexafluorates, J. Electroanal. Chem. 647 (2010) 169–180, http://dx.doi.org/10.1016/j.jelechem.2010.06.006.

[40] R.F. Teoífilo, R. Kiralj, H.J. Ceragioli, A.C. Peterlevitz, V. Baranauskas, L.T. Kubota, et al., QSPR study of passivation by phenolic compounds at platinum and boron-Doped diamond electrodes, J. Electrochem. Soc. 155 (2008) D640, http://dx.doi.org/10.1149/1.2953588.

[41] M.P. Soriaga, A.T. Hubbard, Determination of the orientation of adsorbed molecules at solid-liquid interfaces by thin-layer electrochemistry: aromatic compounds at platinum electrodes, J. Am. Chem. Soc. 104 (1982) 2735–2742, http://dx.doi.org/10.1021/ja00374a008.

[42] R.S. Neves, A.J. Motheo, F.M.S. Silva Fernandes, R.P.S. Fartaria, Monte Carlo simulation of the adsorption of phenol on gold electrodes. A simple model, J. Braz. Chem. Soc. 15 (2004) 224–231.

[43] M.D. Pereda, M. Reigosa, M.A. Fernández Lorenzo, Relationship between radial diffusion of copper ions released from a metal disk and cytotoxic effects. Comparison with results obtained using extracts, Bioelectrochemistry 72 (2008) 94–101, http://dx.doi.org/10.1016/j.bioelechem.2007.11.008.

[44] T. Hall, Specialty metals make sophisticated medical devices possible, in: Med. Des. Briefs, 2013 http://www.medicaldesignbriefs.com/component/content/article/mdb/features/17206.

[45] F. Alvarez, P.L. Schilardi, M.A. Fernández Lorenzo, Reduction of the burst release of copper ions from copper-based intrauterine devices by organic inhibitors, Contraception 85 (2012) 91–98, http://dx.doi.org/10.1016/j.contraception.2011.05.011.

[46] F. Alvarez, C.A. Grillo, P. Schilardi, A. Rubert, G. Benítez, C. Lorente, et al., Decrease in cytotoxicity of copper-based intrauterine devices (IUD) pretreated with 6-mercaptopurine and pterin as biocompatible corrosion inhibitors, ACS Appl. Mater. Interfaces 5 (2013) 249–255, http://dx.doi.org/10.1021/am3025307.

[47] M.B. Petrović Mihajlović, M.M. Antonijević, Copper corrosion inhibitors. period 2008–2014. a review, Int. J. Electrochem. Sci. 10 (2015) 1027–1053, http://dx.doi.org/10.1016/j.ijengsci.2004.12.001.

[48] G. Žerjav, I. Milošev, Protection of copper against corrosion in simulated urban rain by the combined action of benzotriazole, 2-mercaptobenzimidazole and stearic acid, Corros. Sci. 98 (2015) 180–191, http://dx.doi.org/10.1016/j.corsci.2015.05.023.

[49] M. Finšgar, I. Milošev, Inhibition of copper corrosion by 1,2,3-benzotriazole: a review, Corros. Sci. 52 (2010) 2737–2749, http://dx.doi.org/10.1016/j.corsci.2010.05.002.

[50] D. Gelman, D. Starosvetsky, Y. Ein-Eli, Copper corrosion mitigation by binary inhibitor compositions of potassium sorbate and benzotriazole, Corros. Sci. 82 (2014) 271–279, http://dx.doi.org/10.1016/j.corsci.2014.01.028.

[51] B.V. Appa Rao, M. Yakub Iqbal, B. Sreedhar, Self-assembled monolayer of 2-(octadecylthio)benzothiazole for corrosion protection of copper, Corros. Sci. 51 (2009) 1441–1452, http://dx.doi.org/10.1016/j.corsci.2009.03.034.

[52] S. Castro, L.C. Davis, L.E. Erickson, Natural, cost-effective, and sustainable alternatives for treatment of aircraft deicing fluid waste, Environ. Prog. 24 (2005) 26–33, http://dx.doi.org/10.1002/ep.10059.

[53] R. Martinez Palou, O. Olivares-Xomelt, N.V. Likhanova, Environmentally friendly corrosion inhibitors, in: Dev. Corros. Prot., 2014, pp. 431–465.

[54] S. Lin, H. Shih, F. Mansfeld, Corrosion protection of aluminum-Alloys and metal matrix composites by polymer-coatings, Corros. Sci. 33 (1992) 1331–1349.

[55] F. Perreault, R. Popovic, D. Dewez, Different toxicity mechanisms between bare and polymer-coated copper oxide nanoparticles in Lemna gibba, Environ. Pollut. 185 (2014) 219–227, http://dx.doi.org/10.1016/j.envpol.2013.10.027.

[56] H. Bourara, S. Hadjout, Z. Benabdelghani, A. Etxeberria, Miscibility and hydrogen bonding in blends of poly(4-vinylphenol)/Poly(vinyl methyl ketone), Polymers (Basel). 6 (2014) 2752–2763, http://dx.doi.org/10.3390/polym6112752.

[57] L. Guo, H. Sato, T. Hashimoto, Y. Ozaki, FTIR study on hydrogen-bonding interactions in biodegradable polymer blends of poly(3-hydroxybutyrate) and poly(4-vinylphenol), Macromolecules 43 (2010) 3897–3902, http://dx.doi.org/10.1021/ma100307m.

[58] S. Kuo, S. Chan, F. Chang, Miscibility enhancement on the immiscible binary blend of poly (vinyl acetate) and poly (vinyl pyrrolidone) with bisphenol A, Polymer (Guildf) 43 (2002) 1–8.

[59] S.W. Kuo, Hydrogen-bonding in polymer blends, J. Polym. Res. 15 (2008) 459–486, http://dx.doi.org/10.1007/s10965-008-9192-4.

[60] Y.J. Kim, K. Shibata, H. Uyama, S. Kobayashi, Synthesis of ultrahigh molecular weight phenolic polymers by enzymatic polymerization in the presence of amphiphilic triblock copolymer in water, Polymer (Guildf) 49 (2008) 4791–4795, http://dx.doi.org/10.1016/j.polymer.2008.08.065.

[61] I. Poljanšek, M. Krajnc, Characterization of phenol-formaldehyde prepolymer resins by in line FT-IR spectroscopy, Acta Chim. Slov. 52 (2005) 238–244.

[62] G. Socrates (Eds.), Infrared and Raman Characteristic Group Frequencies, John Wiley & Sons Ltd., England, 2004.

[63] W. Simons, Heyden Son (Eds.), The Sadtler Handbook of Infrared Spectra, Sadtler Research Laboratories, Philadelphia, 1978.

[64] R.M. Silverstein, F.X. Webster, D.J. Kiemle, Silverstein – Spectrometric Identification of Organic Compounds, 7th ed., State University of New York, College of Environmental Science and Forestry, 2005.

[65] B. Fei, C. Chen, S. Peng, X. Zhao, X. Wang, L. Dong, FTIR study of poly(propylene carbonate)/bisphenol A blends, Polym. Int. 53 (2004) 2092–2098, http://dx.doi.org/10.1002/pi.1633.

[66] A.G. Al Lafi, FTIR spectroscopic analysis of ion irradiated poly (ether ketone), Polym. Degrad. Stab. 105 (2014) 122–133.

[67] H.X. Nguyen, H. Ishida, Molecular analysis of the melting behaviour of poly(aryl ether ether ketone), Polymer (Guildf) 27 (1986) 1400–1405.

[68] M. Gattrell, D.W. Kirk, A fourier transform infrared spectroscopy study of the passive film produced during aqueous acidic phenol electro- oxidation, J. Electrochem. Soc. 139 (1992) 2736–2744, http://dx.doi.org/10.1149/1.2068972.

[69] M. Ferreira, H. Varela, R.M. Torresi, G. Tremiliosi-Filho, Electrode passivation caused by polymerization of different phenolic compounds, Electrochim. Acta 52 (2006) 434–442, http://dx.doi.org/10.1016/j.electacta.2006.05.025.

[70] D. Fischer, K. Sahre, M. Abdelrhim, B. Voit, V.B. Sadhu, J. Pionteck, et al., Process monitoring of polymers by in-line ATR-IR, NIR and Raman spectroscopy and ultrasonic measurements, C. R. Chim. 9 (2006) 1419–1424, http://dx.doi.org/10.1016/j.crci.2006.06.006.

[71] O. Abbas, C. Rebufa, N. Dupuy, J. Kister, FTIR-Multivariate curve resolution monitoring of photo-Fenton degradation of phenolic aqueous solutions. Comparison with HPLC as a reference method, Talanta 77 (2008) 200–209, http://dx.doi.org/10.1016/j.talanta.2008.06.008.

[72] M.-C. Pham, F. Adami, J. Dubois, An in situ multiple internal reflection fourier transform infrared spectroscopy investigation of the electropolymerization mechanism of substituted phenols on iron electrodes, J. Electrochem. Soc. 134 (1987) 2166–2169.

[73] H.J. Salavagione, J. Arias-Pardilla, J.L. Vázquez, M.C. Miras, E. Morallón, C. Barbero, Spectroelectrochemical study of the oxidation of diaminophenols on platinum electrodes in acidic medium, Electrochim. Acta 50 (2005) 5414–5422, http://dx.doi.org/10.1016/j.electacta.2005.03.022.

[74] G. Nikolic, S. Zlatkovic, M. Cakic, S. Cakic, C. Lacnjevac, Z. Rajic, Fast fourier transform IR characterization of epoxy GY systems crosslinked with aliphatic and cycloaliphatic EH polyamine adducts, Sensors 10 (2010) 684–696, http://dx.doi.org/10.3390/s100100684.